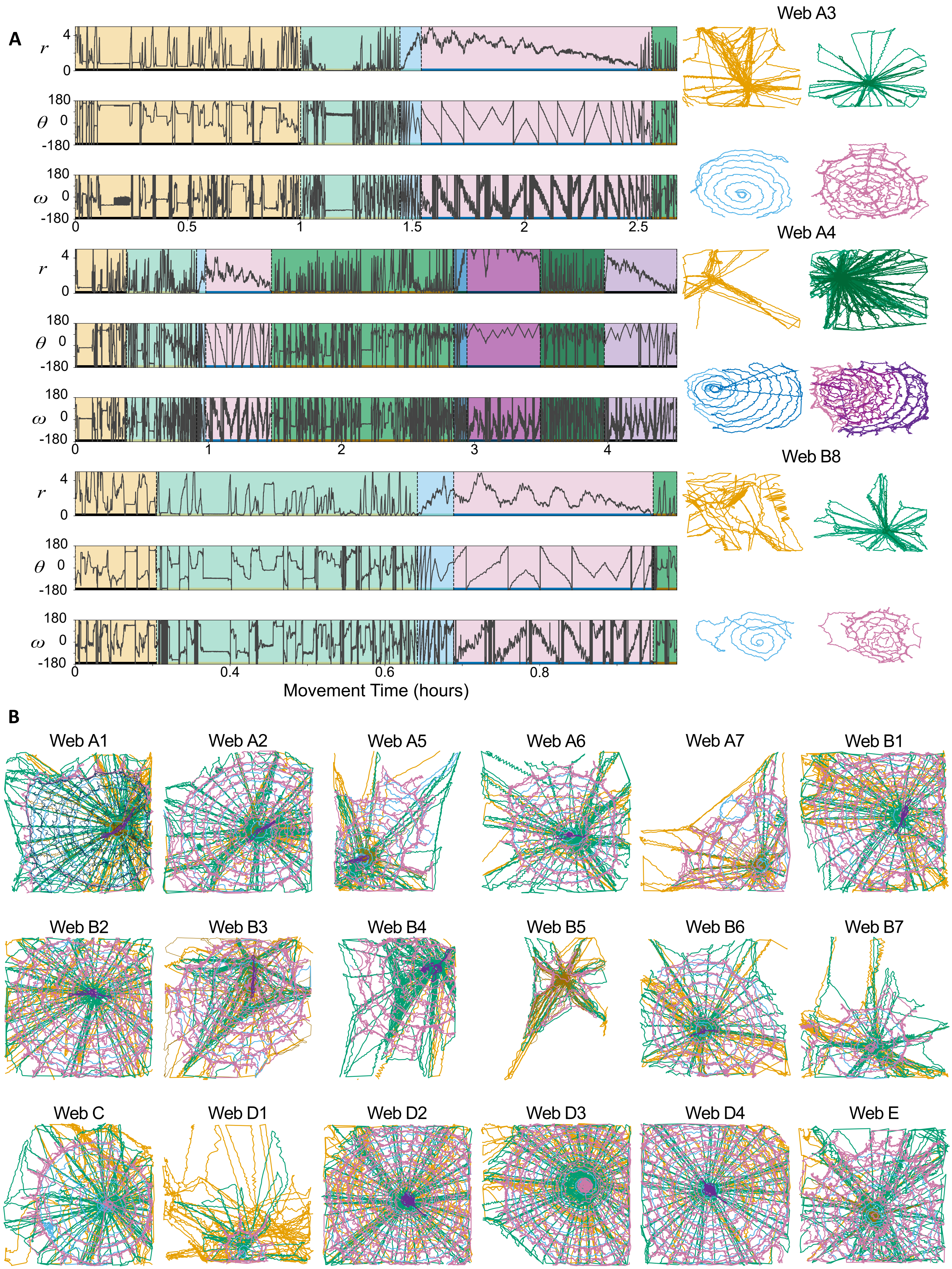
A
Web A3
Web A4
Web B8
r
θ
ω
4
0
180
0
-180
0.5
1
1.5
2
2.5
3
4
0.4
0.6
0.8
Movement Time (hours)
B
Web A1
Web A2
Web A5
Web A6
Web A7
Web B1
Web B2
Web B3
Web B4
Web B5
Web B6
Web B7
Web C
Web D1
Web D2
Web D3
Web D4
Web E

Figure S1. Behavioral diversity and similarity across all 21 recordings, related to Figure 1. (A) Centroid trajectories for three additional recordings. Web stages are highlighted in yellow (protoweb), green (radii), blue (auxiliary spiral), pink (capture spiral), or purple (stabilimentum). **(B)** Coordinates of web progression for the recordings not shown in (A). Webs are named by spider identity (Letters A-E) followed by the order in which each web was constructed over several days (Numbers). Colors are the same as in (A).

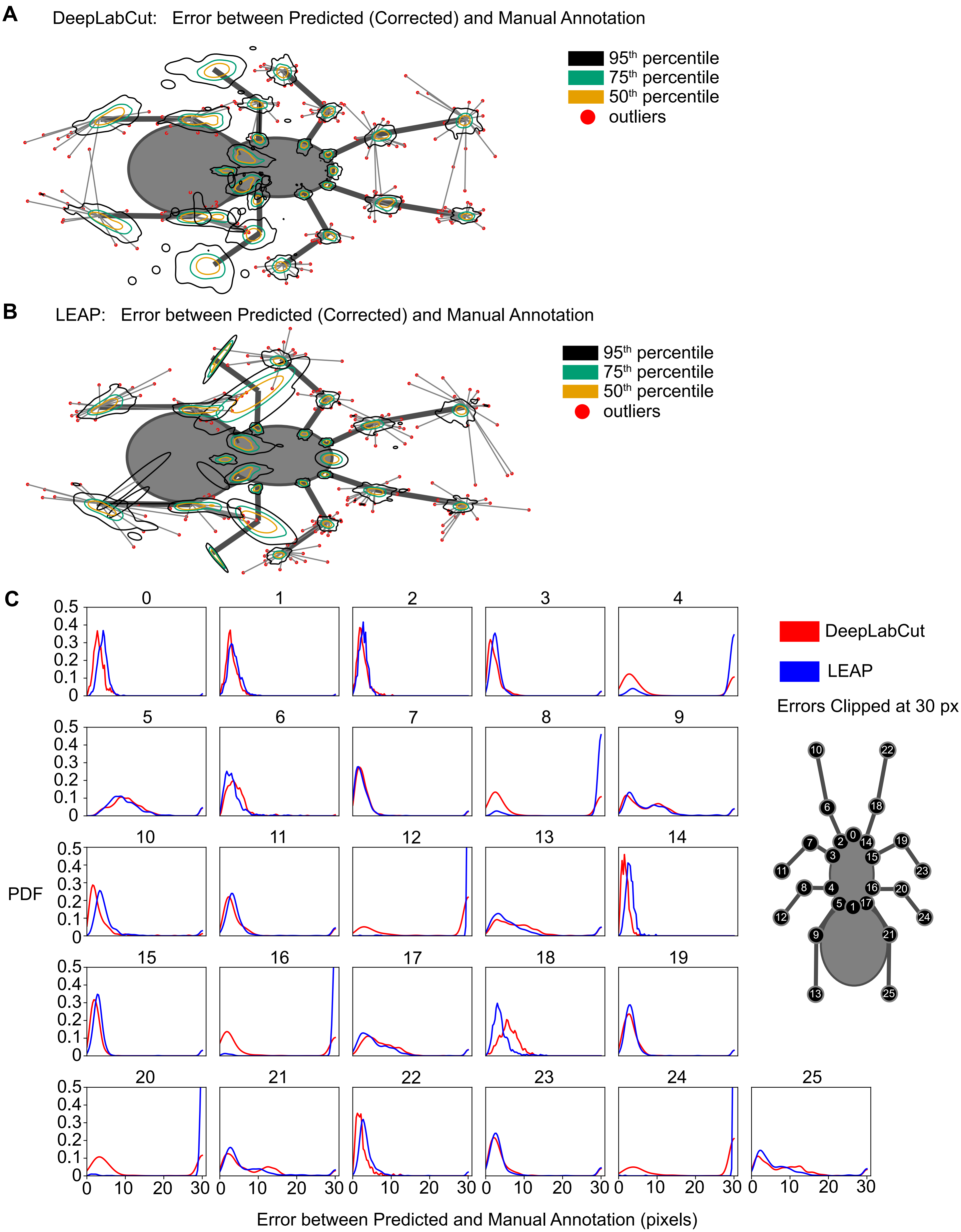
A
DeepLabCut: Error between Predicted (Corrected) and Manual Annotation
95th percentile
75th percentile
50th percentile
outliers
B
LEAP: Error between Predicted (Corrected) and Manual Annotation
95th percentile
75th percentile
50th percentile
outliers
C
DeepLabCut
LEAP
Errors Clipped at 30 px
PDF
Error between Predicted and Manual Annotation (pixels)

Figure S2. Overview of LEAP and DeepLabCut tracking performance, related to Figure 3. (A) DeepLabCut confidence intervals, after limb tracking post-processing, reproduced from (3.A). Tracking error vectors are superimposed onto an arbitrary reference posture. 95th (black), 75th (green) and 50th (yellow) percentile contours are displayed. Errors outside the 95th percentile are displayed as red dots. **(B)** LEAP confidence intervals, after limb tracking post-processing. Tracking error vectors are superimposed onto an arbitrary reference posture. 95th (black), 75th (green) and 50th (yellow) percentile contours are displayed. Errors outside the 95th percentile are displayed as red dots. **(C)** Per-limb coordinate error histogram, before limb tracking post-processing, demonstrating the bimodal error distribution stemming partially from the occurrence of left/right limb confusion. Histograms are titled according to reference coordinates on the spider diagram to the right. PDF = Probability Density Function

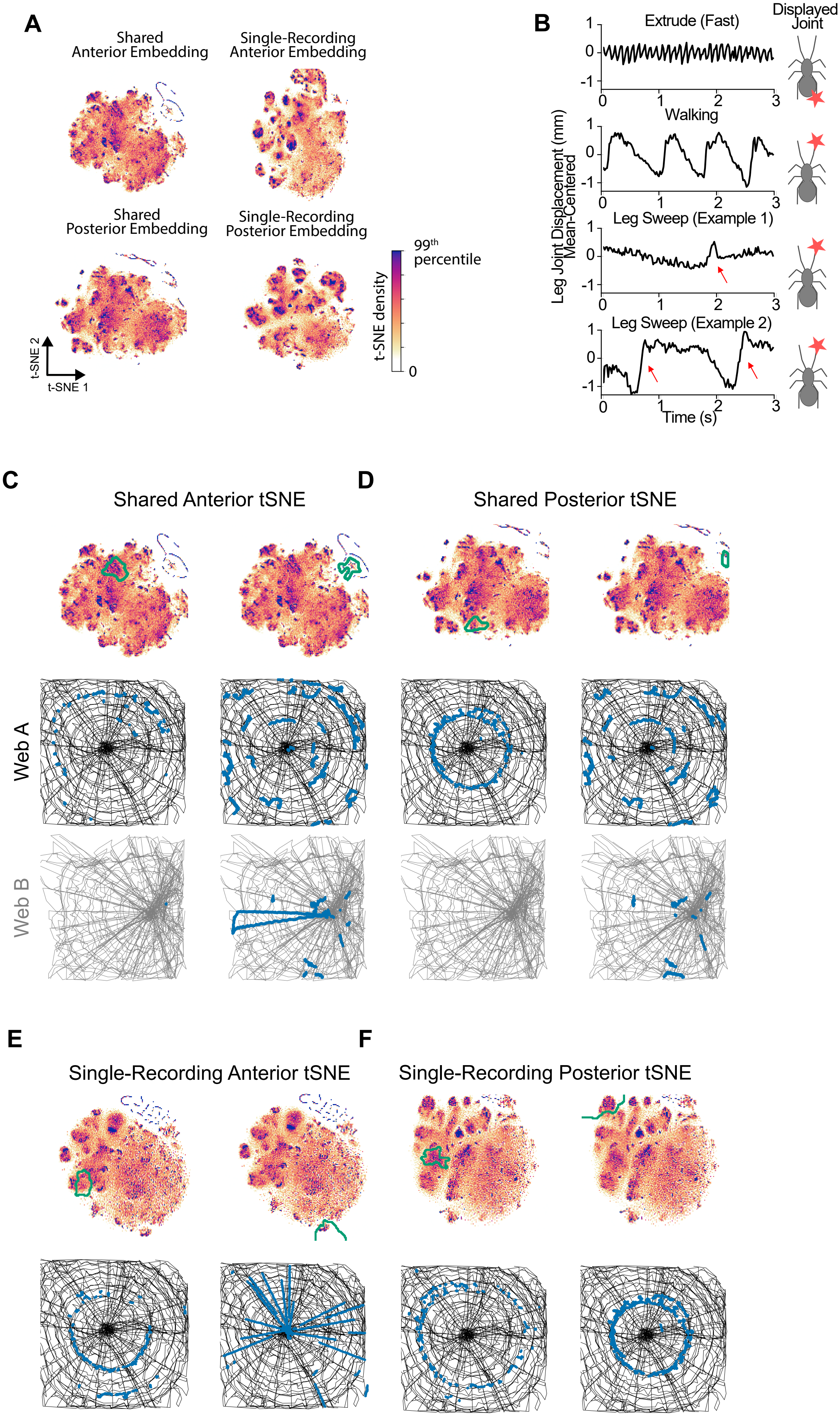
A
Shared Anterior Embedding
Single-Recording Anterior Embedding
Shared Posterior Embedding
Single-Recording Posterior Embedding
99th percentile
t-SNE density
0
t-SNE 2
t-SNE 1
B
Extrude (Fast)
Displayed Joint
Walking
Leg Sweep (Example 1)
Leg Sweep (Example 2)
Leg Joint Displacement (mm) Mean-Centered
Time (s)
C
Shared Anterior tSNE
D
Shared Posterior tSNE
Web A
Web B
E
Single-Recording Anterior tSNE
F
Single-Recording Posterior tSNE

Figure S3. Movement clustering using wavelet embeddings fails to identify shared movement motifs across recordings, related to Figure 3. (A) Shared t-SNE embeddings (Left) versus an individual t-SNE embedding (Right). **(B)** Examples of periodic movements (extrusion, top), occasionally-periodic movements (walking), and non-periodic movement (leg sweep, bottom). **(C)** Top: Movement cluster outlines for two example anterior movement motifs. Bottom: Occurrences of behavioral motifs are highlighted in blue. The centroid history of two different spiders is in black and gray. **(D)** Top: Movement cluster outlines for two example posterior movement motifs. Bottom: Occurrences of behavioral motifs are highlighted in blue. The centroid history of two different spiders is in black and gray. **(E)** Same as C, but for t-SNE embedding obtained from a single recording. **(F)** Same as D, but for t-SNE embedding obtained from a single recording.

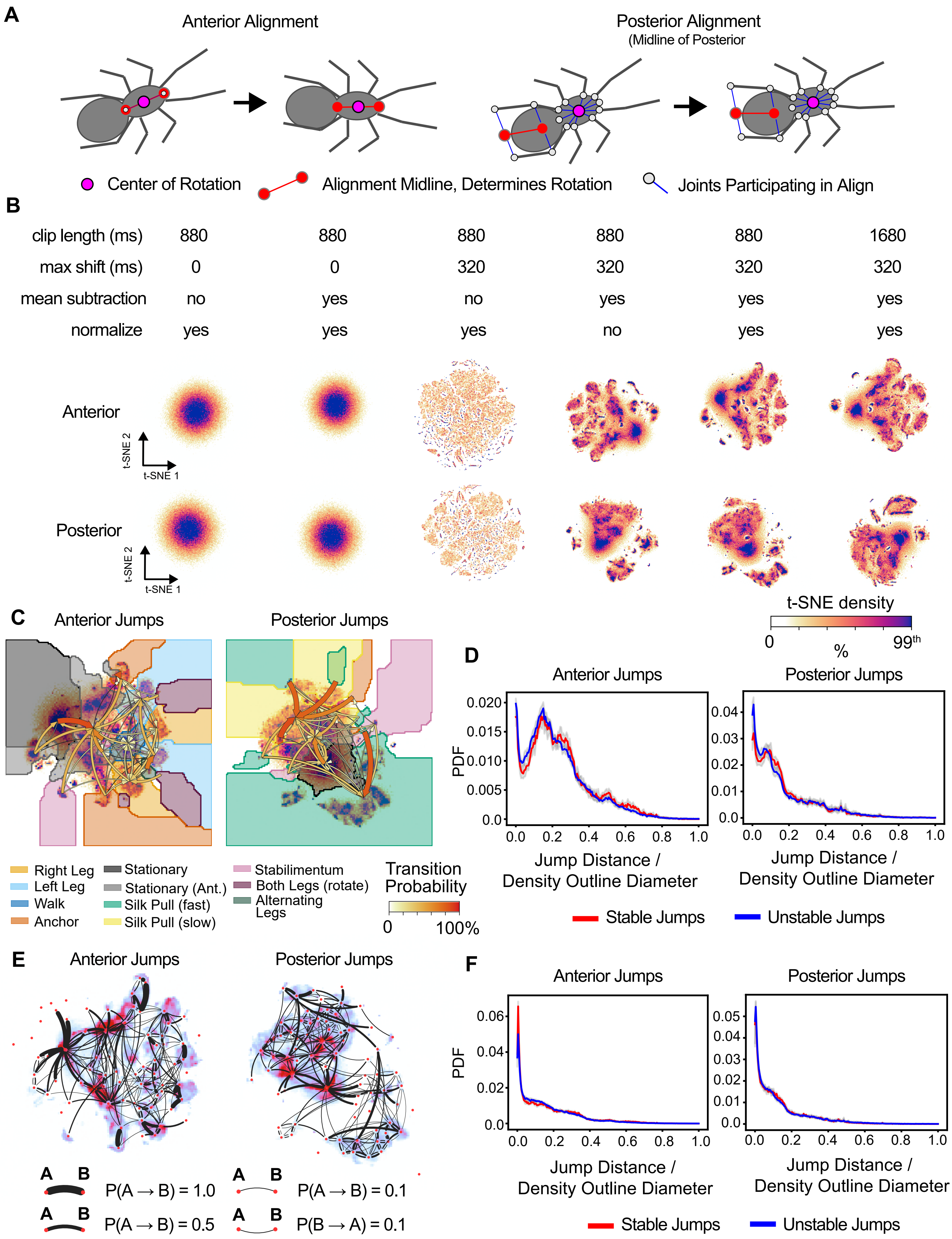

A
Anterior Alignment
Posterior Alignment
(Midline of Posterior
Center of Rotation
Alignment Midline, Determines Rotation
Joints Participating in Align
B
clip length (ms) 880 880 880 880 880 1680
max shift (ms) 0 0 320 320 320 320
mean subtraction no yes no yes yes yes
normalize yes yes yes no yes yes
Anterior
Posterior
t-SNE 1
t-SNE 2
t-SNE density
0 % 99th
C
Anterior Jumps
Posterior Jumps
Right Leg
Left Leg
Walk
Anchor
Stationary
Stationary (Ant.)
Silk Pull (fast)
Silk Pull (slow)
Stabilimentum
Both Legs (rotate)
Alternating Legs
Transition Probability
0 100%
D
Anterior Jumps
Posterior Jumps
PDF
Jump Distance / Density Outline Diameter
Stable Jumps
Unstable Jumps
E
Anterior Jumps
Posterior Jumps
P(A → B) = 1.0
P(A → B) = 0.5
P(A → B) = 0.1
P(B → A) = 0.1
F
Anterior Jumps
Posterior Jumps
PDF
Jump Distance / Density Outline Diameter
Stable Jumps
Unstable Jumps

Figure S4. Posture Alignment Metric (PAM) Methodology and t-SNE Density Transitions, Related to Figure 3. (A) Illustration of the body posture alignment used prior to applying the Posture Alignment Metric (PAM). Anterior leg joints are centered and rotated based on the anterior and posterior thoracic marker. Posterior leg joints are oriented with respect to the midline of posterior limb joints only. **(B)** Overview of anterior and posterior shared t-SNE embeddings obtained with varying temporal and mean-shift parameters, indicating the importance of temporal realignment and mean-subtraction for movement clustering with PAM. **(C)** t-SNE behavior density transitions for anterior and posterior legs. t-SNE densities are defined and colored as in Figure 3E. Arrows indicate transitions between densities, and are colored according to the probability of the transition. Transitions are computed and shown between manually grouped clusters, except that non-contiguous clusters with the same manual annotation are split, in contrast to other analyses. Transitions are normalized such that all outgoing transition probabilities for a given state sum to one. Only transitions with probability ≥ 0.05 are shown. **(D)** Probability density functions for anterior and posterior transition distances as shown in (C). All transition distances are normalized by the diameter of t-SNE space, based on the minimum enclosing circle of all t-SNE bins with a density ≥0.1% of the maximum. Jump distances are defined as the Euclidean distance between temporally adjacent t-SNE coordinates (T_X & T_Y, belonging to manually grouped clusters X and Y, respectively) when $X \neq Y$. Stable jumps are those where T_X is the last position of a sequence within cluster X of length ≥ 12 frames (≥ 240 ms) and T_Y is the first position of a sequence within cluster Y of length ≥ 12 frames. For stable jumps, any positions T_Z occurring after T_X and before T_Y are ignored if they are not part of a sequence within cluster Z of length ≥ 12 frames. Shaded regions represent the 25th-75th percentile range. **(E)** Same as C, but for transitions between watershed-defined clusters. Arc handedness indicates direction as indicated in the legend. **(F)** Same as D, but for transitions between watershed-defined clusters as shown in (E). Only transitions with probability ≥ 0.05 are shown.

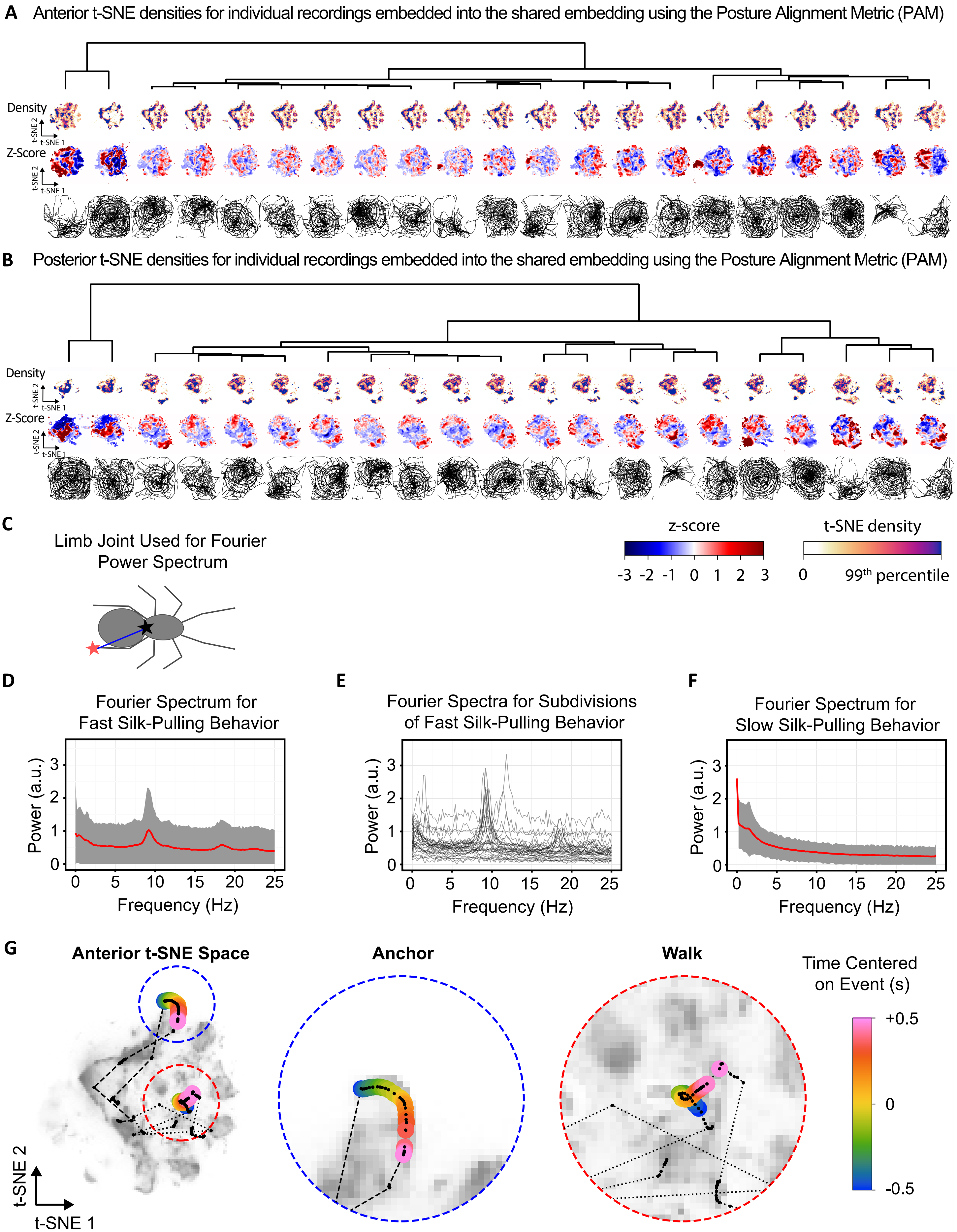

A
Anterior t-SNE densities for individual recordings embedded into the shared embedding using the Posture Alignment Metric (PAM)
Density
Z-Score
t-SNE 1
t-SNE 2
B
Posterior t-SNE densities for individual recordings embedded into the shared embedding using the Posture Alignment Metric (PAM)
Density
Z-Score
t-SNE 1
t-SNE 2
C
Limb Joint Used for Fourier Power Spectrum
z-score
-3 -2 -1 0 1 2 3
t-SNE density
0
99th percentile
D
Fourier Spectrum for Fast Silk-Pulling Behavior
Power (a.u.)
Frequency (Hz)
E
Fourier Spectra for Subdivisions of Fast Silk-Pulling Behavior
Power (a.u.)
Frequency (Hz)
F
Fourier Spectrum for Slow Silk-Pulling Behavior
Power (a.u.)
Frequency (Hz)
G
Anterior t-SNE Space
Anchor
Walk
Time Centered on Event (s)
+0.5
0
-0.5
t-SNE 2
t-SNE 1

Figure S5. **Hierarchical clustering of movement embeddings, related to Figure 3.** **(A)** Hierarchical clustering of anterior movements using the Posture Alignment Metric (PAM). Each of the 21 recordings is displayed as a column, with its density (top), density Z-score with respect to the mean (middle) and web rendering (bottom). Densities are clipped to the 99th percentile before mean, standard deviation and Jensen-Shannon (J-S) distances are computed. Recordings are clustered based on pairwise J-S distances. **(B)** Hierarchical clustering of posterior movements using the Posture Alignment Metric (PAM), as in (A). **(C)** Limb Joint Diagram illustrating limb coordinate used in D-F. Fourier spectra are computed with respect to the displacement (blue line) of the left posterior limb joint (red star) relative to the posterior thoracic marker (black star). **(D)** Fourier Power Spectra of the fast silk pulling behavior. Gray ribbons represent the mean ± standard deviation. **(E)** Fourier Spectra for individual t-SNE subdivisions labelled as “fast silk-pulling” or “combing” behavior. Note the slight heterogeneity that exists in the amplitude and frequency of fast silk-pulling, explaining the subclusters that exist within the movements collectively labeled “fast silk-pulling” (Figure 3E). **(F)** Fourier Power Spectra of the slow silk pulling behavior. Gray ribbons represent the mean ± standard deviation. **(G)** Example trajectories in anterior t-SNE space for the anchoring (blue highlight) and walking (red highlight) behaviors. Trajectory coloring represents time relative to an arbitrary middle time point, defined individually for each example behavior. Black dots represent individual frames, showing 25 t-SNE locations/s.

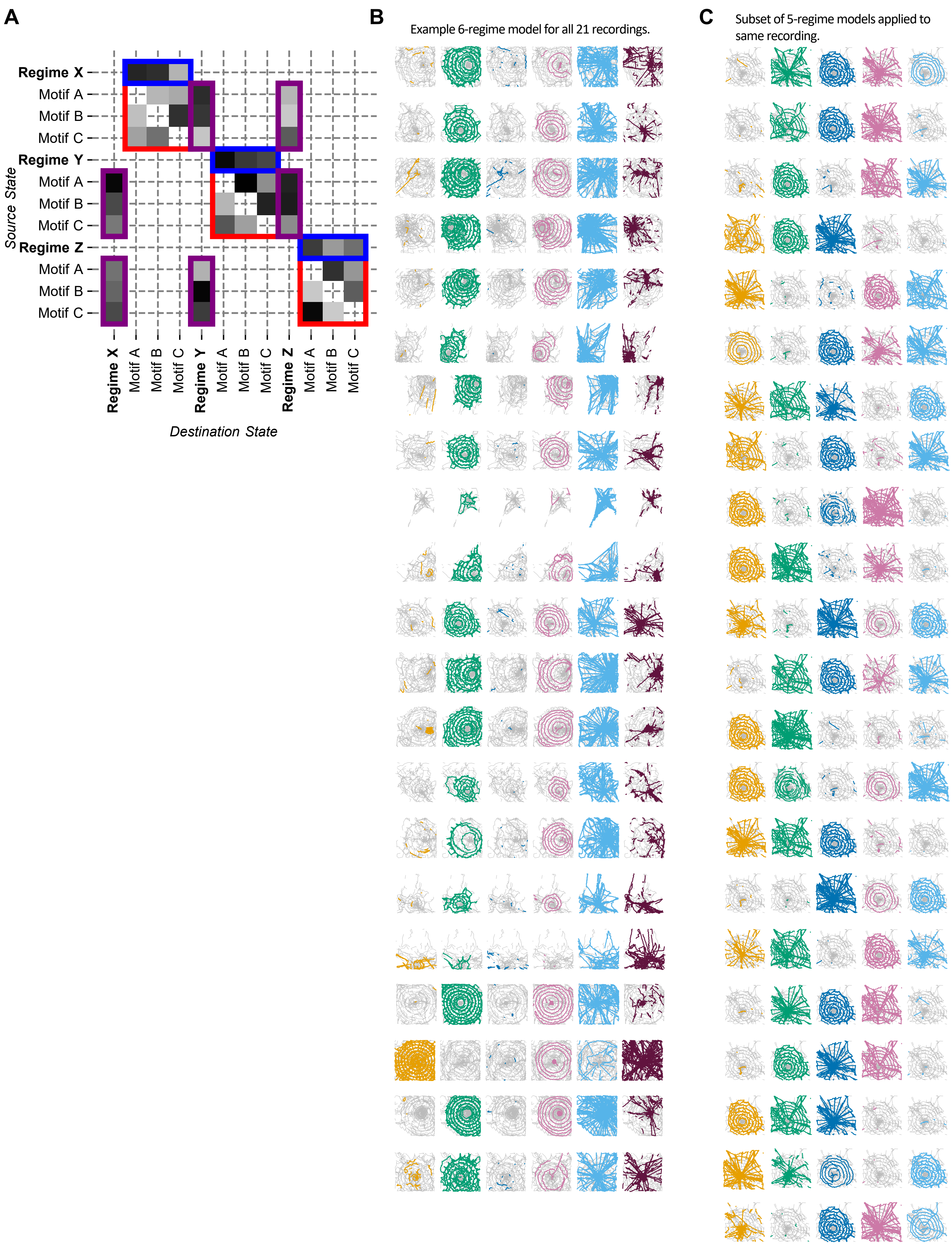
A
Regime X
Motif A
Motif B
Motif C
Regime Y
Motif A
Motif B
Motif C
Regime Z
Motif A
Motif B
Motif C
Source State
Destination State
B
Example 6-regime model for all 21 recordings.
C
Subset of 5-regime models applied to same recording.

Figure S6. Hierarchical Hidden Markov Model (HHMM) structure, related to Figure 6. (A) Example diagram of a Hierarchical Hidden Markov Model (HHMM) implementation as a constrained Hidden Markov Model (HMM). Red squares indicate within-regime transitions. Blue rectangles indicate transitions from hidden parent regime state (with no associated emission) to within-regime movement state. Purple squares indicate transition from a movement state to a parent regime state (with no associated emission). Note that a movement state cannot transition to its own parent regime state, to avoid loops. **(B)** An example 6-regime HHMM, shown for all 21 recordings. **(C)** A subset of 5-regime HHMM models for one recording. Note that only some model instantiations split out the auxiliary spiral stage. This is expected as the model fitting procedure encounters local optima, and models are initialized randomly. The large variation in model performance due to local optima is reflected in the large standard deviation in Figure 6B-C.